Journal of Applied Fluid Mechanics, Vol. 9, No. 1, pp. 379-388, 2016.
Available online at www.jafmonline.net, ISSN 1735-3572, EISSN 1735-3645.
DOI: 10.18869/acadpub.jafm.68.224.24151

Effect of Chemical Reaction on Convective Heat Transfer of Boundary Layer Flow in Nanofluid over a Wedge with Heat Generation/Absorption and Suction

R. M. Kasmani[1], S. Sivasankaran[2 †], M. Bhuvaneswari[2] and Z. Siri[2]

[1] *Centre for Foundation Studies in Science, University of Malaya, Kuala Lumpur 50603, Malaysia*
[2] *Institute of Mathematical Sciences, University of Malaya, Kuala Lumpur 50603, Malaysia*

†*Corresponding Author Email: sd.siva@yahoo.com*

(Received October 12, 2014; accepted January 30, 2015)

ABSTRACT

The aim of the present study is to examine the convective heat transfer of nanofluid past a wedge subject to first-order chemical reaction, heat generation/absorption and suction effects. The influence of wedge angle parameter, thermophoresis, Dufour and Soret type diffusivity are included. The local similarity transformation is applied to convert the governing nonlinear partial differential equations into ordinary differential equations. Shooting method integrated with fourth-order Runge-Kutta method is used to solve the ordinary differential equations. The skin friction, heat and mass transfer rates as well as the effects of various parameters on velocity, temperature and solutal concentration profiles are analyzed. The results indicate that when the chemical reaction parameter increases, the heat transfer coefficient increases while the mass transfer coefficient decreases. The effect of chemical reaction parameter is very important in solutal concentration field compared to velocity and temperature profiles since it decreases the solutal concentration of the nanoparticle.

Keywords: Heat transfer; Nanofluid; Chemical reaction; Thermophoresis.

NOMENCLATURE

a, k_1	constant
C	solutal concentration
C_{fx}	local skin friction
c_p	specific heat
D_{CT}	Soret-type diffusivity
D_S	solutal diffusivity
D_T	thermophoretic diffusion
D_{TC}	dufour-type diffusivity
K_0	chemical reaction coefficient
K^*	chemical reaction parameter
k	thermal conductivity
Le	Lewis number
m	wedge angle parameter
N_{CT}	soret-type parameter
N_T	thermophoresis parameter
N_{TC}	dufour-type parameter
Nu_x	Local Nusselt number
Pr	Prandtl number
Q	heat generation/absorption coefficient
Sh_x	Local Sherwood number
s	suction parameter
T	temperature of the fluid
U	potential flow velocity
u,v	velocity component
v_0	suction velocity
x, y	cartesian coordinates
α	thermal diffusivity
β	hartree pressure gradient
β^*	thermophoretic coefficient
δ	heat generation/absorption parameter
γ	dimensionless concentration
η	similarity variable
μ	dynamic viscosity
ν	kinematic viscosity
θ	dimensionless temperature
ρ	fluid density
τ	ratio of the heat capacity of nanoparticle and heat capacity of the base fluid
ξ	dimensionless distance
ψ	stream function
f	base fluid
p	nanoparticle
w	conditions of the wall
∞	conditions far away from the surface

1. INTRODUCTION

Chemical reactions are classified into two categories; via homogeneous reaction, which involves only single phase reaction and heterogeneous reaction, which involves two or more phases and occur at the interface between fluid and solid or between two fluids separated by an interface. The important applications of homogenous reactions are the combination of common household gas and oxygen to produce a flame and the reactions between aqueous solutions of acids and bases. Themelis (1995) stated that the majority of chemical reactions encountered in applications are first-order and heterogeneous reactions such as hydrolysis of methyl acetate in the presence of mineral acids and inversion of cane sugar in the presence of mineral acids. A chemical reaction is said to be first-order when a reaction rate depends on a single substance and the value of the exponent is one. Midya (2012) observed from their study that the first-order chemical reaction is very important in chemical engineering where the chemical reactions take place between a foreign mass and the working fluid. Bhuvaneswari *et al*. (2009) used Lie group analysis to solve the natural convection heat and mass transfer in an inclined surface with first-order homogenous chemical reaction. Bhattacharyya and Layek (2012) investigated the similarity solution of MHD boundary layer flow with diffusion and chemical reaction over a porous flat plate with suction/blowing. They found that the concentration decreases on increasing the effect of chemical reaction rate. Gangadhar and Reddy (2013) considered the effects of chemically reacting MHD boundary layer flow of heat and mass transfer over a moving vertical plate with suction. Their results revealed that the momentum boundary layer thickness decreases, while both thermal and concentration boundary layer thicknesses increase with an increase in the magnetic field intensity. Uddin *et al*. (2011) used a scaling group of transformations to solve the first order chemical reaction and the variable solute distribution along a stretching surface in the MHD flow of an electrically conducting viscous incompressible fluid. Rout *et al*. (2013) studied the influence of chemical reaction and the effects of heat generation on the laminar boundary layer flow, MHD heat and mass transfer over a moving vertical plate with a convective boundary condition. They discovered that the increase in the strength of chemical reacting substances causes an increase in the magnitude of local skin friction, plate surface temperature and Sherwood number. But, opposite behaviour is observed for local Nusselt number.

The term of nanofluid, introduced by Choi and Eastman (1995), has been particularly fruitful one. Nanofluid is a dispersion of metallic or non-metallic nanometer-sized particles in a liquid resulting in the alteration of the carrier fluid properties such as viscosity, density, and heat transfer capability. Sheikholeslami and Ganji (2014) studied the heated permeable stretching surface in a porous medium using nanofluids and found that choosing Titanium oxide as the nanoparticle and Ethylene glycol as base fluid proved to have the highest cooling performance. Malvandi *et al*. (2014) used the Homotopy Analysis Method to investigate the stagnation point flow of a nanofluid over a porous stretching sheet with heat generation. The study used the Buongiorno model (2006) which identifies the Brownian motion and thermophoresis as the main mechanisms for enhanced convection characteristics of the nanofluid. While studies on nanofluid have been reported extensively in the literature, there are relatively few studies on the chemical reaction effect on mass transfer of nanofluid. Abdul Kahar *et al*. (2011) examined the scaling group transformation for boundary-layer flow of a nanofluid past a porous vertical stretching surface in the presence of chemical reaction with heat radiation. They discovered that the impact of chemical reaction and thermal radiation in the presence of uniform thermophoresis and Brownian diffusion motion have a substantial effect on flow field, heat transfer and nanoparticle volume fraction rate from the sheet to fluid. Later, Kameswaran *et al*. (2012) analyzed the hydromagnetic nanofluid flow due to a stretching or shrinking sheet with viscous dissipation, chemical reaction and Soret effects. They obtained that the mass transfer rate is an increasing function of the chemical reaction parameter in both Cu–water and Ag–water nanofluid. Das (2013) numerically investigated the steady MHD boundary layer flow of an electrically conducting nanofluid past a vertical convectively heated permeable stretching surface with variable stream conditions in presence of chemical reaction. They concluded that the nanoparticle concentration is a decreasing function of chemical reaction parameter.

The study of internal heat generation or absorption is important in problems involving chemical reactions where heat may be generated or absorbed in the course of such reactions. Thus, Rao *et al*. (2012), Chamkha and Ahmed (2011), Magyari and Chamkha (2010) and Mahdy (2010) considered both heat generation or absorption and chemical reaction in their investigations. The effects of thermal radiation and chemical reaction on the MHD fluid flow over a non-linear inclined stretching sheet with variable viscosity in the presence of heat generation/absorption is investigated by Shit and Majee (2014). It is found that the thermal radiation and heat generation/absorption have significant role in controlling the rate of heat transfer in the boundary layer region. Bhuvaneswari *et al*. (2012) examined the radiation natural convection flow of a heat generating fluid over a semi-infinite inclined surface embedded in a porous medium. They found that found that both the velocity and temperature increase on increasing the value of the heat generation parameter. The influence of heat generation or absorption, temperature dependent viscosity and thermal radiation on MHD forced convection over a non-isothermal wedge was investigated by Dal and Mondal (2009). Malleswaran and Sivasankaran (2014) performed a numerical simulation on MHD mixed convection in

a lid-driven cavity with corner heaters. Rahman *et al*. (2012) numerically studied the hydro-magnetic slip flow of water based nanofluid past a wedge with convective surface in the presence of heat generation or absorption. Ashwini and Eswara (2012) examined the MHD Falkner-Skan boundary layer flow with internal heat generation or absorption. They observed that the effect of heat generation or absorption is found to be very significant on heat transfer, but its effect on the skin friction is negligible.

In the past few decades, many studies focus on the boundary layer flow past a wedge. Watanabe (1990) investigated the behavior of boundary layer forced flow over a wedge with uniform suction or injection. Mukhopadhyay presented the radiation effects on boundary layer flow and heat transfer of a fluid with variable viscosity along a symmetric wedge. There are comparatively few studies on 'wedge flow' with the presence of chemical reaction. Kandasamy *et al*. (2008) considered the thermophoresis and chemical reaction effects on non-Darcy mixed convective heat and mass transfer past a porous wedge with variable viscosity in the presence of suction or injection. They found out that the concentration decreases on increasing the values of the chemical reaction parameter due to the presence of first-order chemical reaction. Ganapathirao *et al*. (2013) investigated the non-uniform slot suction/injection on unsteady mixed convection flow over a wedge with chemical reaction and heat generation/absorption. Deka and Sharma (2013) used Falkner-Skan transformations to solve magnetohydrodynamic mixed convection flow past a wedge under variable temperature and chemical reaction.

In the past few years, there are several papers on nanofluid past a wedge, for example, papers by Kasmani *et al*. (2013), Chamkha *et al*. (2012), Yacob *et al*. (2011), Gorla *et al*. (2011) and Khan and Pop (2013). However, none of these papers discussed the effect of chemical reaction on boundary layer flow of nanofluid past a wedge. Thus, the aim of the present paper is to investigate the influence of first-order chemical reaction, internal heat generation/absorption and suction at the wall over a wedge immersed in nanofluid. To the best of author's knowledge, there is no attempt highlighting the above stated flow model for nanofluid.

2. MATHEMATICAL FORMULATION

We consider the two-dimensional, steady, laminar boundary layer flow of nanofluid over a wedge with heat and mass transfer in the presence of internal heat generation/absorption. The velocity components u and v are associated along the $x-$ and $y-$ axis respectively as depicted in the Fig. 1. The first-order chemical reaction is taking place in the flow which moves with the potential flow velocity U. The total angle of the wedge is denoted as Ω, where β is the Hartree pressure gradient. T_w and C_w are the constant temperature and solutal concentration at the wedge wall, T_∞ is the ambient temperature and C_∞ is the solutal concentration of the fluid far away from the wedge. The nanofluid is a dilute solid-liquid mixture with a uniform volume fraction of nanoparticle dispersed within the base fluid. The base fluid and nanoparticles are in thermally equilibrium.

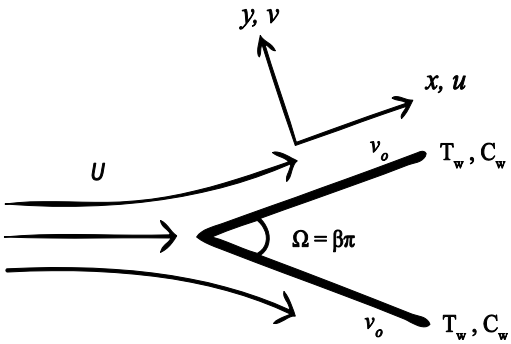

Fig. 1. Flow configuration along the wedge and the coordinate system.

The suction velocity on the wall is considered. Taking the above assumptions into consideration, the governing equations describing momentum, energy and solutal concentration can be written as

$$\frac{\partial u}{\partial x}+\frac{\partial v}{\partial y}=0, \tag{1}$$

$$u\frac{\partial u}{\partial x}+v\frac{\partial u}{\partial y}=\nu\frac{\partial^2 u}{\partial y^2}+U\frac{dU}{dx}, \tag{2}$$

$$u\frac{\partial T}{\partial x}+v\frac{\partial T}{\partial y}=\alpha\frac{\partial^2 T}{\partial y^2}+\tau\left(\frac{D_T}{T_\infty}\right)\left(\frac{\partial T}{\partial y}\right)^2 + D_{TC}\frac{\partial^2 C}{\partial y^2}+Q\left(T-T_\infty\right), \tag{3}$$

$$u\frac{\partial C}{\partial x}+v\frac{\partial C}{\partial y}=D_S\frac{\partial^2 C}{\partial y^2}+D_{CT}\frac{\partial^2 T}{\partial y^2} - K_0\left(C-C_\infty\right), \tag{4}$$

where $\nu=\mu/\rho$ is kinematic viscosity of nanofluid, T is the nanofluid temperature and C is the solutal concentration, $\alpha=k/(\rho c_p)$ is nanofluid thermal diffusivity, $\tau=(\rho c_p)_p/(\rho c_p)_f$ is ratio of the heat capacity of nanoparticle and heat capacity of the base fluid, $D_T=\beta^*\mu C/\rho$ is the thermophoretic diffusion, where $\beta^*=0.26k_f/(2k_f+k_p)$ is the thermophoretic coefficient, D_{TC} is the Dufour-type diffusivity, D_S is the solutal diffusivity, D_{CT} is the Soret-type diffusivity, Q is the heat generation/absorption coefficient and K_0 is the chemical reaction coefficient. The boundary conditions for Eqs. (1) – (4) are expressed as:

$$u = 0,\ v = v_0,\ T = T_w,\ C = C_w \quad \text{at} \quad y = 0, \tag{5}$$

$$u = U,\ T = T_\infty,\ C = C_\infty \quad \text{as} \quad y \to \infty, \tag{6}$$

where v_0 represents the suction velocity at the wall. The mathematical analysis of the problem is simplified by introducing the following quantities:

$$\eta = y\sqrt{\frac{(1+m)U}{2\nu x}},\ \psi = f(\eta)\sqrt{\frac{2U\nu x}{(1+m)}},$$
$$\theta(\eta) = \frac{T - T_\infty}{T_w - T_\infty},\ \gamma(\eta) = \frac{C - C_\infty}{C_w - C_\infty}, \tag{7}$$

where η is the similarity variable, $U = ax^m$ is the potential flow velocity, a is a constant while the exponent m is a wedge angle parameter and m is a function of β such that $m = \beta/(2-\beta) \geq 0$. The stream function $\psi(x,y)$ is defined as $u = \partial\psi/\partial y$ and $v = -\partial\psi/\partial x$. It automatically satisfies the continuity Eq. (1). Therefore, upon using these variables, the governing Eqs. (2) – (4) can be written as

$$\frac{\partial^3 f}{\partial \eta^3} + f\frac{\partial^2 f}{\partial \eta^2} + \frac{2m}{(m+1)}\left(1 - \left(\frac{\partial f}{\partial \eta}\right)^2\right) = \frac{2x}{(m+1)}\left(\frac{\partial^2 f}{\partial x \partial \eta}\frac{\partial f}{\partial \eta} - \frac{\partial^2 f}{\partial \eta^2}\frac{\partial f}{\partial x}\right), \tag{8}$$

$$\frac{\partial^2 \theta}{\partial \eta^2} + \Pr f\frac{\partial \theta}{\partial \eta} + N_T\left(\frac{\partial \theta}{\partial \eta}\right)^2 + N_{TC}\frac{\partial^2 \gamma}{\partial \eta^2} + \Pr\frac{2}{(m+1)}x\frac{Q}{U}\theta = \Pr\frac{2x}{(m+1)}\left(\frac{\partial f}{\partial \eta}\frac{\partial \theta}{\partial x} - \frac{\partial f}{\partial x}\frac{\partial \theta}{\partial \eta}\right), \tag{9}$$

$$\frac{\partial^2 \gamma}{\partial \eta^2} + \mathrm{LePr}\, f\frac{\partial \gamma}{\partial \eta} + N_{CT}\mathrm{Le}\frac{\partial^2 \theta}{\partial \eta^2} - \mathrm{LePr}\frac{2x}{(m+1)}\frac{K_0}{U}\gamma = \frac{2x}{(m+1)}\mathrm{LePr}\left(\frac{\partial f}{\partial \eta}\frac{\partial \gamma}{\partial x} - \frac{\partial f}{\partial x}\frac{\partial \gamma}{\partial \eta}\right), \tag{10}$$

with the following boundary conditions

$$\frac{f}{2}\left(\frac{1}{2}\frac{x}{U}\frac{dU}{dx} + 1\right) + x\frac{\partial f}{\partial x} = s,\quad \frac{\partial f}{\partial \eta} = 0,\ \ \theta = 1,\ \ \gamma = 1, \quad \text{at} \quad \eta = 0, \tag{11}$$

$$f \to 1,\ \ \theta \to 0,\ \ \gamma \to 0, \quad \text{as} \quad \eta \to \infty. \tag{12}$$

The parameters that appeared in the above equations are define as follows: $N_T = \tau D_T (T_w - T_\infty)/\alpha T_\infty$ is the thermophoresis parameter, $\Pr = \nu/\alpha$ is the Prandtl number, $\mathrm{Le} = \alpha/D_S$ is the Lewis number, $N_{TC} = D_{TC}(C_w - C_\infty)/\alpha(T_w - T_\infty)$ is the Dufour parameter, $N_{CT} = D_{CT}(T_w - T_\infty)/\alpha(C_w - C_\infty)$ is the Soret parameter and $s = -v_0\sqrt{(m+1)x/2\nu U}$ is the parameter of suction when $v_0 < 0$ and $s = -v_0\,\mathrm{Re}_x^{1/2}/U$ is the suction parameter and $\mathrm{Re}_x = Ux/\nu$ is the Reynolds number.

Consider the general transformation of independent variables in the Eqs. (8) – (12) from (x,y) to (ξ,η) where $\xi = k_1 x^{(1-m)/2}$ is the dimensionless distance along the wedge with k_1 is constant and $\xi > 0$ (Kafoussias and Nanousis, 1997). The system of Eqs. (8) – (12) can also be written as

$$\frac{\partial^3 f}{\partial \eta^3} + f\frac{\partial^2 f}{\partial \eta^2} + \frac{2m}{(m+1)}\left(1 - \left(\frac{\partial f}{\partial \eta}\right)^2\right) = \frac{1-m}{(m+1)}\xi\left(\frac{\partial f}{\partial \eta}\frac{\partial^2 f}{\partial \xi \partial \eta} - \frac{\partial f}{\partial \xi}\frac{\partial^2 f}{\partial \eta^2}\right) \tag{13}$$

$$\frac{\partial^2 \theta}{\partial \eta^2} + \Pr f\frac{\partial \theta}{\partial \eta} + N_T\left(\frac{\partial \theta}{\partial \eta}\right)^2 + N_{TC}\frac{\partial^2 \gamma}{\partial \eta^2} + \Pr\frac{2}{(m+1)}\xi^2\delta\theta = \Pr\frac{1-m}{(m+1)}\xi\left(\frac{\partial f}{\partial \eta}\frac{\partial \theta}{\partial \xi} - \frac{\partial f}{\partial \xi}\frac{\partial \theta}{\partial \eta}\right) \tag{14}$$

$$\frac{\partial^2 \gamma}{\partial \eta^2} + \mathrm{LePr}\, f\frac{\partial \gamma}{\partial \eta} + N_{CT}\mathrm{Le}\frac{\partial^2 \theta}{\partial \eta^2} - \mathrm{LePr}\frac{2}{(m+1)}\xi^2 K^*\gamma = \mathrm{LePr}\frac{1-m}{m+1}\xi\left(\frac{\partial f}{\partial \eta}\frac{\partial \phi}{\partial \xi} - \frac{\partial f}{\partial \xi}\frac{\partial \phi}{\partial \eta}\right) \tag{15}$$

$$\frac{1}{2}(m+1)f + \frac{1-m}{2}\xi\frac{\partial f}{\partial \xi} = s,\quad f' = 0,\ \ \theta = 1,\ \ \gamma = 1, \quad \text{at} \quad \eta = 0, \tag{16}$$

$$f \to 1,\ \ \theta \to 0,\ \ \gamma \to 0, \quad \text{as} \quad \eta \to \infty. \tag{17}$$

where $\delta = Q/k_1^2 a$ is the heat generation/absorption parameter and $K^* = K_0/k_1^2 a$ is the chemical reaction parameter. It may be observed that if either ξ or derivative with respect to ξ remain in the transformed Eqs. (13) – (17), similarity solutions will not exist. However, when dropping the terms containing partial derivatives with respect to ξ and retaining ξ as a parameter, this approach is called local similarity assumption. The resulting solutions is generally valid if ξ and (or) the discarded values of $\partial f/\partial \xi$ and $\partial f'/\partial \xi$ are small (Kays and Crowford, 1980). Thus, the local similarity solutions of Eqs. (13) – (15) subjected to the appropriate boundary conditions (16) – (17) is obtained by deleting the terms containing partial derivatives with respect to ξ, and considers ξ as a parameter. By employing this assumption, Eqs. (13) – (15) reduce to

$$f''' + ff'' + \frac{2m}{(m+1)}\left(1 - f'^2\right) = 0 \tag{18}$$

$$\theta'' + \Pr f\theta' + N_T\theta'^2 + N_{TC}\gamma'' + \Pr\frac{2}{(m+1)}\xi^2\delta\theta = 0 \quad (19)$$

$$\gamma'' + \mathrm{Le}\Pr f\gamma' + \mathrm{Le}N_{CT}\theta'' - \mathrm{Le}\Pr\frac{2}{(m+1)}\xi^2K^*\gamma = 0 \quad (20)$$

with the boundary conditions

$$f = 2s/(m+1),\quad f' = 0,\ \theta = 1,\ \gamma = 1, \quad \text{at} \quad \eta = 0, \quad (21)$$

$$f \to 1,\ \theta \to 0,\ \gamma \to 0, \quad \text{as} \quad \eta \to \infty., \quad (22)$$

where prime denotes the partial differentiation with respect to η. The physical quantities of primary interest are the local skin-friction coefficient C_{fx}, the local Nusselt number Nu_x and the local Sherwood number Sh_x which are dezfined as

$$C_{fx}\left(\mathrm{Re}_x\right)^{1/2} = \left((m+1)/2\right)^{1/2} f''(0), \quad (23)$$

$$Nu\left(\mathrm{Re}_x\right)^{-1/2} = -\left((m+1)/2\right)^{1/2}\theta'(0) \quad (24)$$

$$Sh(\mathrm{Re}_x)^{-1/2} = -\left((m+1)/2\right)^{1/2}\gamma'(0) \quad (25)$$

3. NUMERICAL SOLUTION

The nonlinear ordinary differential Eqs. (18) – (20) along with boundary conditions (21) – (22) are the two point boundary value problem. These equations are converted to an initial value problem and reduced to first order system as follows:

$$f = f_1,\ f' = f_2,\ f'' = f_3,\quad \theta = \theta_1,\ \theta' = \theta_2,\quad \gamma = \gamma_1,\ \gamma' = \gamma_2, \quad (26)$$

$$f''' = -f_1f_3 - \frac{2m}{(m+1)}\left(1 - f_2f_2\right), \quad (27)$$

$$\theta'' = -\Pr f_1\theta_2 - N_T\theta_2\theta_2 - N_{TC}\gamma'' + \Pr\frac{2}{(m+1)}\xi^2\delta\theta_1, \quad (28)$$

$$\gamma'' = -\mathrm{Le}\Pr f_1\gamma_2 - N_{CT}\mathrm{Le}\theta'' + \mathrm{Le}\Pr\frac{2}{(m+1)}\xi^2K^*\gamma_1, \quad (29)$$

with boundary conditions

$$f_1(0) = 2s/(m+1),\ f_2(0) = 0,\quad \theta_1(0) = 1,\ \gamma_1(0) = 1. \quad (30)$$

The values for $f_3(0), \theta_2(0)$ and $\gamma_2(0)$ are needed for solving the Eqs. (27) – (29). Since the three values are unknown, the initial guesses for $f_3(0), \theta_2(0)$ and $\gamma_2(0)$ are chosen. Then, the fourth-order Runge-Kutta method is used to obtain the solution from $\eta = 0$ to a suitable finite value of $\eta \to \infty$, say $\eta = \eta_\infty$. In this paper, the step size $\Delta\eta$ is taken as 0.01 and η_∞ is selected to vary from 7 to 15, depending on the physical parameters. The guessed values are refined systematically by shooting method until all boundary conditions, $f'(\eta_\infty) = 1,\ \theta(\eta_\infty) = 0$ and $\gamma(\eta_\infty) = 0$ are satisfied. The values of $f_3(0), \theta_2(0)$ and $\gamma_2(0)$ are adjusted by Newton-Raphson method for getting better numerical approximation. A convergence criteria based on the absolute relative difference between the current and the previous iteration values is employed within a pre-assigned tolerance, $\varepsilon <= 10^{-5}$. If the difference meets the convergence criteria, the solution is assumed to have converged and the iterative process is terminated.

An examination of the present data with those available in the literature has been done in order to verify the accuracy of the present computer code. Table 1 shows the comparison of skin friction and heat transfer coefficients for different values of m when $N_T, N_{TC}, N_{CT}, \delta, K^*$ and s are set to be zero with Watanabe (1990). It can be seen from the Table 1 that the agreement between the results is excellent. This gives the confident on our numerical computations.

Table 1 Comparison of skin friction and heat transfer coefficients for various values of m when

$\Pr = 0.73,\ N_T = N_{TC} = N_{CT} = \delta = K^* = \mathrm{Le} = s = 0$

m	$f''(0)$		$-\theta'(0)$	
	Watanabe (1990)	Present	Watanabe (1990)	Present
0.0435	0.56898	0.56898	0.43548	0.43548
0.0909	0.65498	0.65498	0.44730	0.44730
0.1429	0.73200	0.73200	0.45693	0.45694
0.2000	0.80213	0.80213	0.46503	0.46503
0.3333	0.92765	0.92765	0.47814	0.47814

4. RESULTS AND DISCUSSION

The impact of all physical parameters on the skin friction, heat and mass transfer rates is given in Table 2 and Table 3. The Prandtl number for the base fluid (water) is fixed as $\Pr = 6.2$ in all numerical computations. It is observed from Table 2 that the skin friction rate increases on increasing the wedge angle and suction parameter. The velocity gradient near the wedge surface is larger when suction is present and the wedge angle parameter increases. This result is consistent with the physical interpretation of the skin friction, which $f''(0)$ represents the velocity gradient at the wedge surface and is also related to the drag coefficient on the wall. However, the skin friction coefficient remains unchanged when the value of N_T, N_{TC}, N_{CT}, δ and K^* are changing because those parameters appear only in the energy and solutal concentration equations. The heat transfer rate shows an increasing pattern when the values of all the parameters are increasing except suction

parameter. The heat transfer rate decreases on increasing the suction parameter. Therefore, the thermal boundary layer thickness becomes small for the increase of the suction parameter. It is observed that the rate of mass transfer increases as the value of m increases. The mass transfer rate decreases when $N_T, N_{TC}, N_{CT}, \delta, s$ and K^* increase as depicted in Table 3.

Table 2 The skin friction, heat transfer and mass transfer coefficients for various values of m and s when

$N_T = N_{TC} = N_{CT} = 0.1, \delta = K^* = 0.2,$ Le $= 5$.

m	s	$f''(0)$	$-\theta'(0)$	$-\gamma'(0)$
0.0909	0.5	1.34053	3.25008	2.42073
0.2000		1.39035	2.94983	2.34354
0.3333		1.43445	2.65698	2.26229
0.5000		1.47391	2.37305	2.17555
0.5	0.3	1.04808	1.66310	2.46897
	0.7	1.64951	4.80176	2.50337
	0.9	1.97053	6.32726	2.61619
	1.2	2.46814	8.58918	2.94566

Table 3 The skin friction, heat transfer and mass transfer coefficients for various values of N_T, N_{TC}, N_{CT}, δ, K^* when $m = 0.0909, s = 0.5$ and Le $= 5$.

N_T	N_{TC}	N_{CT}	δ	K^*	$-\theta'(0)$	$-\gamma'(0)$
0.3	0.1	0.1	0.2	0.2	2.17362	0.25197
0.5					1.43882	0.62505
0.7					0.93610	2.22326
0.1	0.1	0.1	0.2	0.2	3.25008	2.42073
	0.3				1.44491	4.81450
	0.5				0.52777	5.11516
0.1	0.1	0.3	0.2	0.2	1.37060	5.14912
		0.5			0.90375	5.33196
		0.7			0.58135	5.38980
0.1	0.1	0.1	-0.6	0.2	4.60890	1.06391
			-0.4		4.31299	1.35946
			-0.2		3.99280	1.67933
			0.4		2.80191	2.86763
			0.8		1.59676	4.06722
			1.0		0.64325	5.01408
0.1	0.1	0.1	0.2	0.5	3.16473	3.21696
				1.0	3.06087	4.28092
				1.3	3.01328	4.81374

Figure 2 shows the dimensionless velocity, temperature and solutal concentration profiles for different values of wedge angle, m. The value of $m = 0(0°)$ corresponds to the boundary layer flow past a flat horizontal surface whereas $m = 0.3333(90°)$ corresponds to the boundary layer flow past a vertical plate. It is observed from Fig. 2 that the fluid velocity increases as the wedge angle parameter m increases. The results also show that the velocity profiles became steeper for larger values of the wedge angle. In addition, the velocity profiles squeeze closer and closer to the surface of the wall, thus the hydrodynamic boundary layer becomes thin as m increases. It is clear from this figure that both temperature and solutal concentration profiles increase on increasing the values of wedge angle.

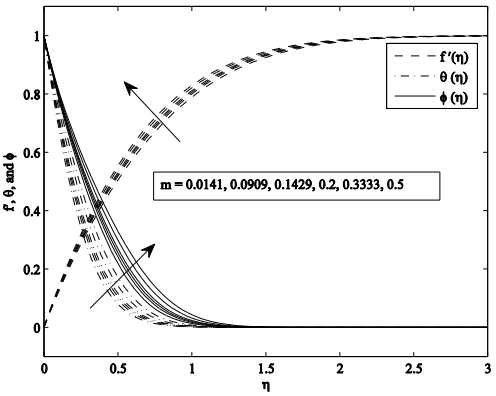

Fig. 2. The velocity, temperature and solutal concentration profiles for different values of m when

$N_T = N_{TC} = N_{CT} = 0.1, \delta = 0.2, K^* = 0.2, s = 0.5$ **and** Le $= 5$.

The influence of Dufour, thermophoresis and Soret parameters are depicted in Fig. 3(a), 3(b) and 3(c), respectively. The temperature profile shows an increasing pattern when all parameters increase. This means that the thermophoresis N_T, Dufour N_{TC} and Soret N_{CT} parameters work to increase the values of temperature in the fluid and then decrease the gradient at the wall and it results an increase thickness of the thermal boundary layer. The solutal concentration profile shows a decreasing behaviour when the Dufour parameter increases but the opposite result is obtained for thermophoresis and Soret parameters. This fact indicates that the Dufour parameter reduces the nanoparticle diffusion while the thermophoresis and Soret parameters enhance the nanoparticle diffusion.

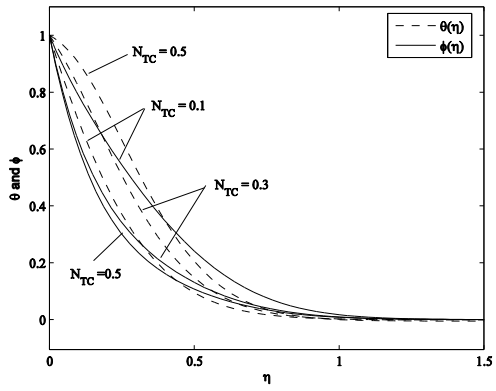

Fig. 3(a). The temperature and solutal concentration profiles for different values of N_{TC} when

$N_T = N_{CT} = 0.1, m = 0.0909, \delta = 0.2, K^* = 0.2,$
$s = 0.5$ **and** Le $= 5$.

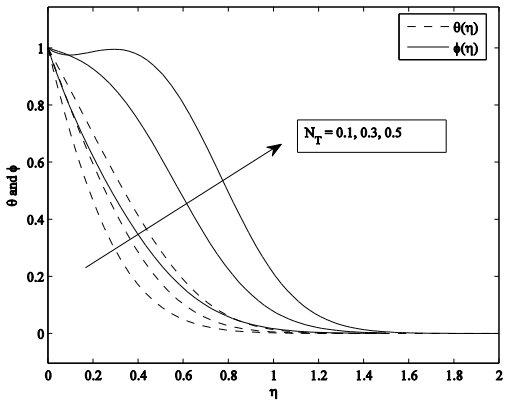

Fig. 3(b). The temperature and solutal concentration profiles for different values of N_T when
$N_{TC} = N_{CT} = 0.1$, $m = 0.0909$, $\delta = 0.2$, $K^* = 0.2$, $s = 0.5$ **and** $\mathrm{Le} = 5$ **.**

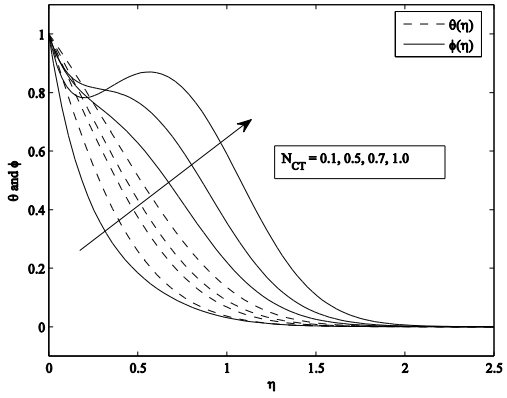

Fig. 3(c). The temperature and solutal concentration profiles for different values of N_{CT} when
$N_T = N_{TC} = 0.1$, $m = 0.0909$, $\delta = 0.2$, $K^* = 0.2$, $s = 0.5$ **and** $\mathrm{Le} = 5$ **.**

Figures 4(a) and 4(b) present the effect of heat generation/absorption for temperature and solutal concentration profiles, respectively. The positive values of δ indicate heat generation (source) and negative values of δ correspond to heat absorption (sink). It is noted that the temperature of nanofluid increases with the increase of δ. Therefore, the thermal boundary layer thickness becomes large when decreasing the heat source/sink parameter. This is expected since heat generation causes the thermal boundary layer to become thicker and the temperature of the fluid to increase, whereas the opposite effect with heat absorption reducing temperature of the fluid and the thermal buoyancy effect. The solutal concentration profile decreases with an increase of δ when $\eta < 0.5$. However, when η is approximately greater than 0.5 ($\eta > 0.5$), the solutal concentration of the nanoparticles shows an increasing pattern.

Figure 5 depicts the influence of chemical reaction on the dimensionless temperature and solutal concentration profiles with the fixed values of other parameters. It is obvious that an increase in the chemical reaction parameter results a decreasing in the solutal concentration profile. The distribution of solutal concentration becomes weak in the presence of chemical reaction. So, the solutal concentration boundary layer becomes thin as the chemical reaction parameter increases. From Fig. 5, it is observed that the chemical reaction influences the solutal concentration field. However, it has a minor effect on thermal diffusion. This explains the minor influence of chemical reaction on temperature profile. It is worth mentioning here that, the large values of K^* shows small changes on temperature field.

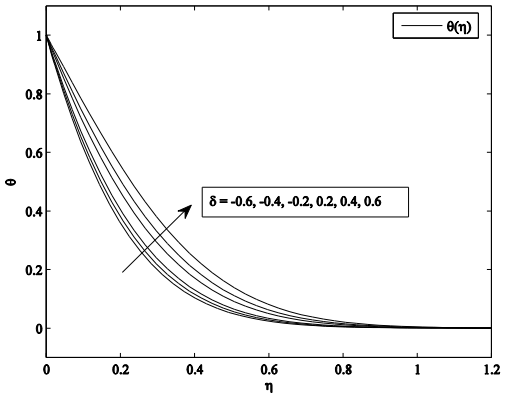

Fig. 4(a). The temperature profile for different values of δ when $N_T = N_{TC} = N_{CT} = 0.1$,
$m = 0.0909$, $K^* = 0.2$, $s = 0.5$ **and** $\mathrm{Le} = 5$ **.**

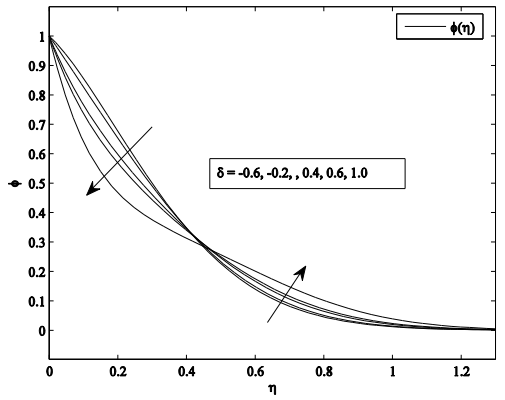

Fig. 4(b). The solutal concentration profile for different values of δ when
$N_T = N_{TC} = N_{CT} = 0.1$,
$m = 0.0909$, $K^* = 0.2$, $s = 0.5$ **and** $\mathrm{Le} = 5$ **.**

Figure 6 displays the velocity, temperature and solutal concentration profiles against η for various values of suction parameter ($s > 0$). It can be seen from the figure that the velocity of the fluid increases with an increase of suction velocity, that is, the fluid particles gains velocity on increasing the suction value. Therefore, the thicknesses of the hydrodynamic and thermal boundary layers are found to decrease with the increase of suction parameter. It is clear that increasing the suction parameter tends to decrease the temperature of the

fluid as well as the solutal concentration of nanoparticles. The imposition of suction at wedge surface reduces the region of viscous domination close to the wall, which causes decreasing in the fluid's temperature as well as the solutal concentration profiles.

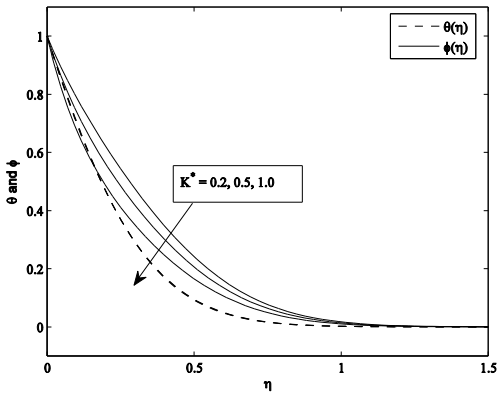

Fig. 5. The temperature and solutal concentration profiles for different values of K^* when $N_T = N_{TC} = N_{CT} = 0.1$, $m = 0.0909$, $\delta = 0.2$, $s = 0.5$ and $\mathrm{Le} = 5$.

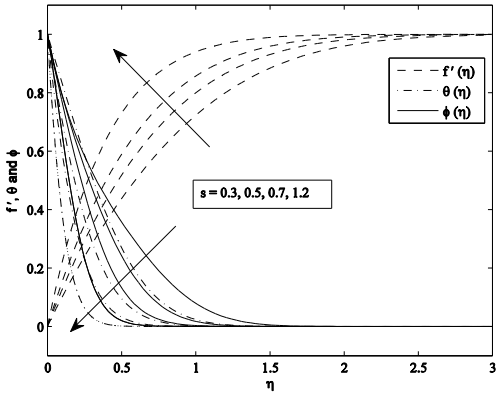

Fig. 6. The velocity, temperature and solutal concentration profiles for different values of s when $N_T = N_{TC} = N_{CT} = 0.1$, $m = 0.0909$, $\delta = 0.2$, $K^* = 0.2$ and $\mathrm{Le} = 5$.

5. CONCLUSION

The problem of boundary layer flow of nanofluid along a wedge in the presence of first-order chemical reaction, heat generation/absorption and suction effects has been investigated. The conclusions from the present study are as below:

- The velocity of the fluid increases with m and s, however it remains unchanged on increasing the values of N_T, N_{TC}, N_{CT}, δ and K^*.
- The temperature increases with m, N_T, N_{TC}, N_{TC} and δ and it decreases on increasing K^* and s.
- Solutal concentration increases with m, N_T and N_{CT} and it decreases with an increase in N_{TC}, δ, s and K^*.
- The skin friction coefficient increases on increasing the suction and wedge angle parameters. The thermophoresis, Dufour, Soret, heat generation or absorption and chemical reaction parameters have no effect on flow field, therefore they have no effect on skin friction coefficient.
- The heat transfer rate increases on increasing wedge angle, chemical reaction, thermophoresis, Dufour and Soret parameters. However, it decreases on increasing the suction value.
- The mass transfer enhances by increasing the wedge angle. The mass transfer decreases on increasing the thermophoresis, Dufour, Soret, heat generation/absorption, suction and chemical reaction parameters.

ACKNOWLEDGEMENTS

The authors thank to University of Malaya for financial support under University Malaya Research Grants: RG216-12AFR, RP011B-13AFR and RP010C-13AFR.

REFERENCES

Abdul-Kahar, R., R. Kandasamy and I. Muhaimin (2011). Scaling group transformation for boundary-layer flow of a nanofluid past a porous vertical stretching surface in the presence of chemical reaction with heat radiation. *Computers & Fluids* 52, 15–21.

Ashwini, G. and A. T. Eswara (2012). MHD Falkner-Skan boundary layer flow with internal heat generation or absorption. *World Academy of Science, Engineering and Technology* 65, 662–665.

Bhattacharyya, K. and G. C. Layek (2012). Similarity solution of MHD boundary layer flow with diffusion and chemical reaction over a porous flat plate with suction/blowing. *Meccanica* 47, 1043–1048.

Bhuvaneswari, M., S. Sivasankaran and M. Ferdows (2009). Lie group analysis of natural convection heat and mass transfer in an inclined surface with chemical reaction. *Nonlinear Analysis: Hybrid Systems* 3, 536–542.

Bhuvaneswari, M., S. Sivasankaran and Y. J. Kim (2012). Lie group analysis of radiation natural convection flow over an inclined surface in a porous medium with internal heat generation. *Journal of Porous Media* 15(12), 1155-1164.

Buongiorno, J. (2006). Convective transport in nanofluids. *Journal of Heat Transfer* 128, 240–250.

Chamkha, A. J. and S. E. Ahmed (2011). Similarity solution for unsteady MHD flow near a stagnation point of a three-dimensional porous body with heat and mass transfer, heat generation/absorption and chemical reaction. *Journal of Applied Fluid Mechanics* 4(2), 87–94.

Chamkha, A. J., S. Abbasbandy, A. M. Rashad and K. Vajravelu (2012). Radiation effects on mixed convection over a wedge embedded in a porous medium filled with a nanofluid. *Transport in Porous Media* 91, 261–279.

Das, K. (2013). Lie group analysis for nanofluid flow past a convectively heated stretching surface. *Applied Mathematics and Computation* 221, 547–557.

Deka, R. K. and S. Sharma (2013). Magnetohydrodynamic mixed convection flow past a wedge under variable temperature and chemical reaction. *American Journal of Computational and Applied Mathematics* 3(2), 74–80.

Gangadhar, K. and N. B. Reddy (2013). Chemically reacting MHD boundary layer flow of heat and mass transfer over a moving vertical plate in a porous medium with suction. *Journal of Applied Fluid Mechanics* 6(1), 107–114.

Gorla, R. S. R., A. J. Chamkha and A. M. Rashad (2011). Mixed convective boundary layer flow over a vertical wedge embedded in a porous medium saturated with a nanofluid: Natural convection dominated regime. *Nanoscale Research Letters* 6, 207.

Kafoussias N. G and N. D. Nanousis (1997). Magnetohydrodynamic laminar boundary layer flow over a wedge with suction or injection. *Canadian Journal of Physics* 75, 733–745.

Kameswaran, P. K., M. Narayana, P. Sibanda and P. V. S. N. Murthy (2012). Hydromagnetic nanofluid flow due to a stretching or shrinking sheet with viscous dissipation and chemical reaction effects. *International Journal of Heat and Mass Transfer* 55, 7587–7595.

Kandasamy, R., I. Muhaimin, I. Hashim and R. M. Kasmani (2008). Thermophoresis and chemical reaction effects on non-Darcy mixed convective heat and mass transfer past a porous wedge with variable viscosity in the presence of suction or injection. *Nuclear Engineering and Design* 238, 2699–2705.

Kasmani, R. M., I. Muhaimin and R. Kandasamy (2013). Laminar boundary layer flow of a nanofluid along a wedge in the presence of suction/injection. *Journal of Applied Mechanics and Technical Physics* 54(3), 377–384.

Kays, W. M. and M. E. Crawford (1980). *Convective heat and mass transfer*. McGraw-Hill Book Company.

Khan, W. A. and I. Pop (2013). Boundary layer flow past a wedge moving in a nanofluid. *Mathematical Problems in Engineering* 2013, 637285.

Magyari, E. and A. J. Chamkha (2010). Combined effect of heat generation or absorption and first-order chemical reaction on micropolar fluid flows over a uniformly stretched permeable surface: The full analytical solution. *International Journal of Thermal Sciences* 49, 1821–1828.

Mahdy, A. (2010). Effect of chemical reaction and heat generation or absorption on double-diffusive convection from a vertical truncated cone in porous media with variable viscosity. *International Communications in Heat and Mass Transfer* 37, 548–554.

Malleswaran, A. and S. Sivasankaran (2016). Numerical simulation on MHD mixed convection in a lid-driven cavity with corner heaters. *Journal of Applied Fluid Mechanics* 9(4).

Malvandi, A., F. Hedayati and M. R. H. Nobari (2014). An HAM analysis of stagnation-point flow of a nanofluid over a porous stretching sheet with heat generation. *Journal of Applied Fluid Mechanics* 7(1), 135–145.

Midya, C. (2012). Exact solutions of chemically reactive solute distribution in MHD boundary layer flow over a shrinking surface. *Chinese Physics Letters* 29, 014701.

Mukhopadhyay, S. (2009). Effects of radiation and variable fluid viscosity on flow and heat transfer along a symmetric wedge. *Journal of Applied Fluid Mechanics* 2(2), 29–34.

Pal, D. and H. Mondal (2009). Influence of temperature-dependent viscosity and thermal radiation on MHD forced convection over a non-isothermal wedge. *Applied Mathematics and Computation* 212, 194–208.

Rahman, M. M., M. A. Al-Lawatia, I. A. Eltayeb and N. Al-Salti (2012). Hydromagnetic slip flow of water based nanofluids past a wedge with convective surface in the presence of heat generation (or) absorption. *International Journal of Thermal Sciences* 57, 172–182.

Rao, J. A., S. Sivaiah and R. S. Raju (2012). Chemical reaction effects on an unsteady MHD free convection fluid flow past a semi-infinite vertical plate embedded in a porous medium with heat absorption. *Journal of Applied Fluid Mechanics* 5(3), 63–70.

Rout, B. R., S. K. Parida and S. Panda (2013). MHD heat and mass transfer of chemical

reaction fluid flow over a moving vertical plate in presence of heat source with convective surface boundary condition. *International Journal of Chemical Engineering* 2013, 296834.

Sheikholeslami, M. and D. D. Ganji (2014). Heated permeable stretching surface in a porous medium using nanofluids. *Journal of Applied Fluid Mechanics* 7(3), 535–542.

Shit, G. C. and S. Majee (2014). Hydromagnetic flow over an inclined non-linear stretching sheet with variable viscosity in the presence of thermal radiation and chemical reaction. *Journal of Applied Fluid Mechanics* 7(2), 239–247.

Themelis, N. J. (1995). *Transport and chemical rate phenomena*. Taylor & Francis Group.

Uddin, M. S., K. Bhattacharyya, G. C. Layek and W. A. Pk (2011). Chemically reactive solute distribution in a steady MHD boundary layer flow over a stretching surface. *Journal of Applied Fluid Mechanics* 4(4), 53–58.

Watanabe, T. (1990). Thermal boundary layer over a wedge with uniform suction or injection in forced flow. *Acta Mechanica* 83, 119–126.

Yacob, N. A., A. Ishak, R. Nazar and I. Pop (2011). Falkner–Skan problem for a static and moving wedge with prescribed surface heat flux in a nanofluid. *International Communications in Heat and Mass Transfer* 38, 149–153.